Catal Lett (2007) 119:217–221
DOI 10.1007/s10562-007-9243-1

Synthesis of Nanowire TiO_2 Thin Films by Hydrothermal Treatment and their Photoelectrochemical Properties

Masaaki Kitano · Ryo Mitsui · Diana Rakhmawaty Eddy · Zeinhom M. A. El-Bahy · Masaya Matsuoka · Michio Ueshima · Masakazu Anpo

Received: 19 June 2007 / Accepted: 5 August 2007 / Published online: 7 September 2007

Abstract Nanowire TiO_2 thin films were successfully prepared on Ti metal substrates by hydrothermal treatment of calcined Ti foils in 10 M NaOH. The nanowire TiO_2 thin films exhibited much larger surface area and higher photoelectrochemical performance than the TiO_2 thin films prepared on Ti metal substrates by the calcination of Ti foil. These nanowire films were shown to act as an efficient photoanodes for the photoelectrochemical water splitting reaction.

Keywords TiO_2 nanowire thin film · Photocatalyst · Hydrothermal synthesis · Water splitting

1 Introduction

Titanium oxide (TiO_2) materials have been extensively investigated in areas such as photocatalysis and solar cells due to such advantages as their low cost, high photocatalytic reactivity and chemical stability [1–3]. It is known that various factors, such as its particle size [4–6], surface area [7], and crystallinity [7–10], affect the photocatalytic activity of TiO_2. Therefore, the precise control of these parameters can be considered essential in obtaining highly active TiO_2 photocatalysts. Since the pioneering work of Kasuga et al. [11, 12] in which TiO_2 nanotubes were prepared by the simple one-step hydrothermal treatment of TiO_2 crystals with a NaOH aqueous solution, various studies on the synthesis of nanostructured TiO_2, such as nanotubes [13–15], nanowires [16, 17], and nanofibers [18], have been carried out. However, most of the nanostructured TiO_2 prepared by hydrothermal treatment are obtained in powder form of neither anatase nor rutile phase [13, 17, 18] and are difficult to handle for practical or industrial use [19, 20]. Therefore, these TiO_2 materials exhibit low photocatalytic activity. The development of nanostructured TiO_2 thin films with good crystallinity would, therefore, be of great importance not only as effective photocatalysts but also for such applications as gas sensors, photovoltaic cells, high surface area electrodes, etc. Along these lines, we have successfully prepared nanowire TiO_2 thin films by hydrothermal treatment of calcined Ti foil in NaOH aqueous solution. These films were shown to exhibit a remarkable enhancement in the photoelectrochemical oxidation of water under UV light irradiation [21]. Moreover, Yang et al. [22] have also reported the formation of rutile nanotube-like TiO_2 electrodes using a similar method.

In the present work, nanowire TiO_2 thin films have been prepared by a simple hydrothermal treatment and their characteristics, photoelectrochemical properties, and photocatalytic activities for the water splitting reaction have been investigated.

2 Experimental

2.1 Preparation of TiO_2 nanowire thin films

TiO_2 thin films (TiO_2/Ti) were prepared on a Ti metal substrate by calcining Ti metal foil of 0.25 mm thickness at

---

M. Kitano · M. Ueshima
Industry-University Cooperation Organization, Osaka Prefecture University, 1-2 Gakuen-cho, Naka-ku, Sakai, Osaka 599-8570, Japan

R. Mitsui · D. R. Eddy · Z. M. A. El-Bahy · M. Matsuoka · M. Anpo (✉)
Department of Applied Chemistry, Graduate School of Engineering, Osaka Prefecture University, 1-1 Gakuen-cho, Naka-ku, Sakai, Osaka 599-8531, Japan
e-mail: anpo@chem.osakafu-u.ac.jp

873 K for 5 h in air. These TiO_2 thin films were then subjected to reactions with 10 M NaOH aqueous solution in a Teflon-lined stainless autoclave and kept for 12–72 h at 393 K. After cooling to room temperature (rt), the films were washed in 0.1 M HCl solution and nanowire TiO_2 thin films were obtained. These nanowire films were referred to as nw-TiO_2(*X*)/Ti, where *X* is the time (h) of hydrothermal treatment.

2.2 Photoelectrochemical Measurements

The photoelectrochemical properties of the TiO_2 thin film electrodes were evaluated using a potentiostat (HZ3000, Hokuto Denko). The three-electrode cell consisted of the TiO_2 thin film electrode, a Pt electrode and a saturated calomel electrode (SCE) as the working, counter and reference electrodes, respectively. The working electrode was irradiated from the front side (light incident on the electrolyte/electrode interface) by a 500 W Xe lamp or 500 W high pressure Hg lamp in 0.25 M K_2SO_4 solution which was mechanically stirred and purged with 99.99% pure Ar gas before and during the experiment. The area of the working electrode exposed to light was about 0.2 cm^2. The incident photon to current conversion efficiency (IPCE), defined as the number of electrons collected per incident photon, was determined by measuring the photocurrent (I_{ph}) of the electrodes at each excitation wavelength and by using the following equation [23, 24]:

$$\mathrm{IPCE}(\%) = \{[1240 \times I_{\mathrm{ph}}(\mathrm{A/cm^2})]/[\lambda(\mathrm{nm}) \times I_{\mathrm{inc}}(\mathrm{W/cm^2})]\} \times 100$$

where I_{inc} is the incident light intensity (W/cm^2), and λ is the excitation wavelength (nm). Light irradiation was carried out using a 500 W Xe arc lamp with an interference filter (λ_{max} = 360 nm, half width: 22.9 nm). The incident light intensity (I_{inc}) was measured by a laser power meter (I_{inc} = 435 μW/cm^2).

2.3 Photoelectrochemical Reactions

The separate evolution of H_2 and O_2 from water was investigated using an H-type Pyrex glass container connected to a vacuum system (10^{-3} Pa) and the detailed experimental procedures are described in previous literature [25, 26]. The back side of TiO_2/Ti or nw-TiO_2(*X*)/Ti where the Ti metal surface is exposed was deposited with Pt by a radio frequency (RF) magnetron sputtering deposition method with an RF power of 70 W under a substrate temperature of 298 K. These Pt-loaded TiO_2 thin films were referred to as TiO_2/Ti/Pt and nw-TiO_2(*X*)/Ti/Pt. The container consists of two water phases separated by a TiO_2 thin film and proton-exchange membrane (Nafion film). Prior to the reaction, the reaction cell was de-aerated by purging with 99.99% pure Ar gas for 3 h. Light irradiation was carried out with a 500 W Xe arc lamp through the reaction cell and the evolved H_2 and O_2 were analyzed by a gas chromatograph (GC, G2800-T, Yanaco) with a thermal conductivity detector (TCD).

2.4 Characterizations

The crystal structure of the TiO_2 thin films was investigated by X-ray diffractometer analysis (XRD, XRD-6100, Shimadzu). The morphologies of the TiO_2 thin films were observed by scanning electron microscopy (SEM, S-4500, Hitachi) and the surface compositions of the TiO_2 thin films were obtained by X-ray photoelectron spectroscopy (XPS, ESCA-3200, Shimadzu).

3 Results and Discussions

Figure 1 shows the SEM images of the TiO_2/Ti thin films before and after hydrothermal treatment in 10 M NaOH aqueous solution. After 12 h hydrothermal treatment, the nanowire structures could be partially observed on the Ti substrate. The nw-TiO_2(24)/Ti exhibited complicated surface structures consisting of the numerous stacking of nanowires having a diameter of around 30–50 nm and showing a remarkable contrast to TiO_2/Ti which has a smooth flat surface. Furthermore, it was found that the XPS spectra of the nw-TiO_2(*X*)/Ti thin films show only the peaks assigned to Ti 2p and O 1s and no peak assigned to Na 1s, showing that Na^+ ions are effectively removed by washing with HCl aqueous solution after hydrothermal treatment (data not shown).

The effect of hydrothermal treatment on the surface area of the TiO_2/Ti thin films was investigated by BET surface measurements using krypton gas as the adsorbate. As summarized in Table 1, the surface area of the TiO_2/Ti thin film increased as the time of hydrothermal treatment increased. The surface area of nw-TiO_2(48)/Ti was 15 times larger than that of TiO_2/Ti. Figure 2 shows the XRD patterns of the TiO_2/Ti and nw-TiO_2(*X*)/Ti thin films. The TiO_2/Ti film shows XRD peaks due to the Ti metal and rutile phase, while the peak intensity of the rutile phase for the nw-TiO_2(*X*)/Ti films decreased depending on the length of hydrothermal treatment. It has been reported that nanotube materials obtained by the reaction of TiO_2 powder with concentrated NaOH are composed of a layered titanate, such as $Na_xH_{2-x}Ti_3O_7$, $H_2Ti_4O_9 \cdot H_2O$, $H_2Ti_2O_4(OH)_2$, etc., rather than anatase or rutile phase TiO_2 [13, 17,

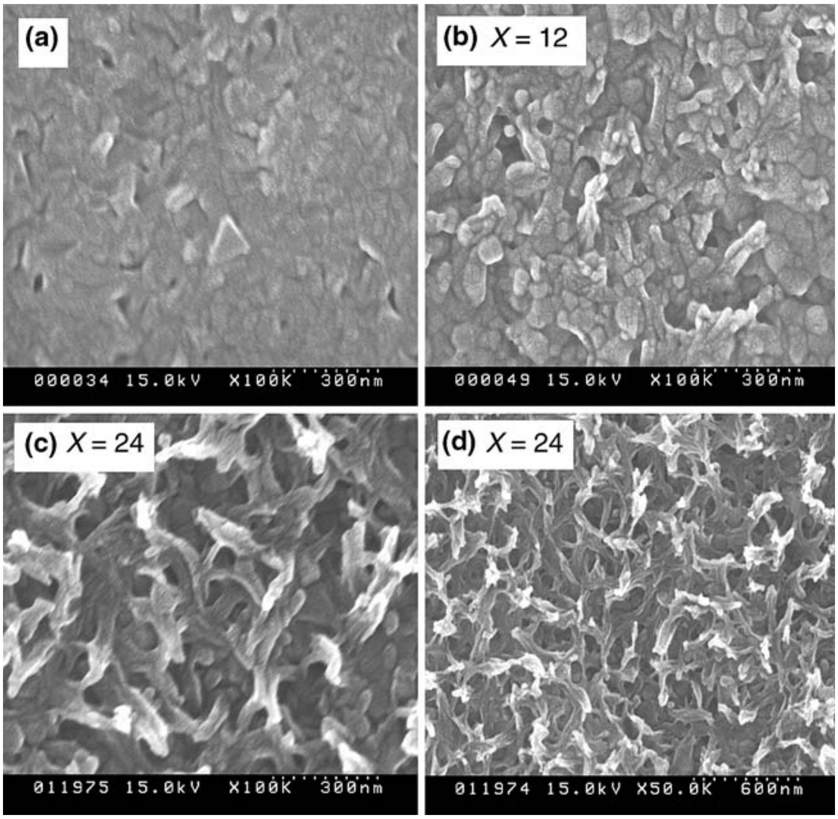

Fig. 1 SEM images of (**a**) TiO_2/Ti and (**b–d**) nw-TiO_2(*X*)/Ti thin films. The (**d**) image shows a lower magnification image of (**c**)

Table 1 Surface areas of TiO_2/Ti and nw-TiO_2(*X*)/Ti thin films

Sample	$A^{a}_{bet}(cm^2)$
TiO_2/Ti	26
nw-TiO_2(12)/Ti	80
nw-TiO_2(24)/Ti	167
nw-TiO_2(48)/Ti	414
nw-TiO_2(72)/Ti	428

[a] Sample size: 5 × 20 mm^2

18]. However, nw-TiO_2(*X*)/Ti thin films show no XRD peak at around $2\theta = 10°$ due to the layered titanate.

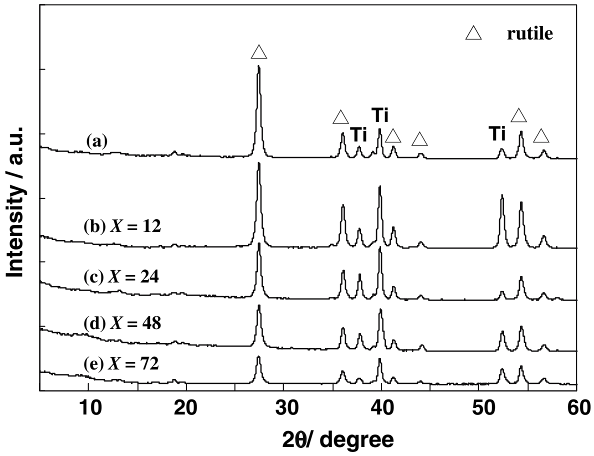

Fig. 2 XRD patterns of (**a**) TiO_2/Ti and (**b–e**) nw-TiO_2(*X*)/Ti thin films

Nanostructured TiO_2 films are photoactive as they undergo charge separation when subjected to the following band gap excitation (1):

$$TiO_2 + hv \rightarrow TiO_2(e_{CB} + h_{VB}) \quad (1)$$

where e_{CB} and h_{VB} represent the conduction band electrons and valence band holes, respectively. The photogenerated electrons can be readily collected at the conducting surface in a photoelectrochemical cell [23, 27]. Photoelectrochemical measurements were performed using a standard three-electrode system consisting of a working electrode (TiO_2/Ti, nw-TiO_2(*X*)/Ti), Pt wire counter electrode and SCE reference electrode in an Ar-purged 0.25 M K_2SO_4 aqueous solution. Figure 3 shows the current–potential curves of the TiO_2/Ti and nw-TiO_2(*X*)/Ti electrodes. Dark currents were negligible under scanning potentials of –0.5 to +1.5 V vs. SCE, while the anodic photocurrent increased with an increase in the anodic bias. The observed photocurrent represents the anodic oxidation of water to oxygen by the photogenerated holes at the nw-TiO_2(*X*)/Ti film electrode under UV light irradiation. Moreover, it can be seen that the photocurrent increased with an increase in the treatment time, reaching a plateau at 48 h and suggesting that nw-TiO_2(X)/Ti electrodes exhibit much higher photocurrent than the TiO_2/Ti electrode. The nw-TiO_2(X)/Ti films have the advantage of having a short diffusion length of the photoformed holes in the bulk to surface. Moreover, the electrolyte solution can penetrate into the interspaces throughout the film. The incident photons are also more efficiently absorbed on film having a rough surface than a flat one since light trapping through scattering at the surface of the structure is enhanced on a rough surface [28]. In order to investigate the stability of nw-TiO_2(48)/Ti, current–potential curves were measured repeatedly under irradiation with the full arc of a 500 W high pressure Hg lamp. Although the anodic photocurrent slightly decreased with repeated scanning, it approached a saturated value of around 7.5 mA after 1 h. These results suggest that the nanowire structure is kept stable during the reaction and the photocurrent is not based on the oxidation of nw-TiO_2(48)/Ti itself but on the oxidation of water. In fact, no noticeable changes in the SEM images nw-TiO_2(48)/Ti before or after photoelectrochemical measurements could be observed. Figure 4 shows the photocurrents observed for the TiO_2/Ti and nw-TiO_2(48)/Ti electrode as a function of the wavelengths controlled by the cut-off filters. Light irradiation was carried out with a 500 W Xe arc lamp. As shown in Fig. 4, the nw-TiO_2(48)/Ti electrode exhibited a higher photocurrent than the TiO_2/Ti electrode and the onset of the photocurrent for both nw-TiO_2(48)/Ti and TiO_2/Ti electrode was observed at a wavelength of around 400–410 nm, corresponding to the energy gaps for rutile, 3.0 eV. The incident photon to current conversion efficiencies (IPCE) of TiO_2/Ti and nw-TiO_2(48)/Ti electrode under UV light irradiation (λ = 360 nm) were determined to be 13.1 % and 23.7 %, respectively.

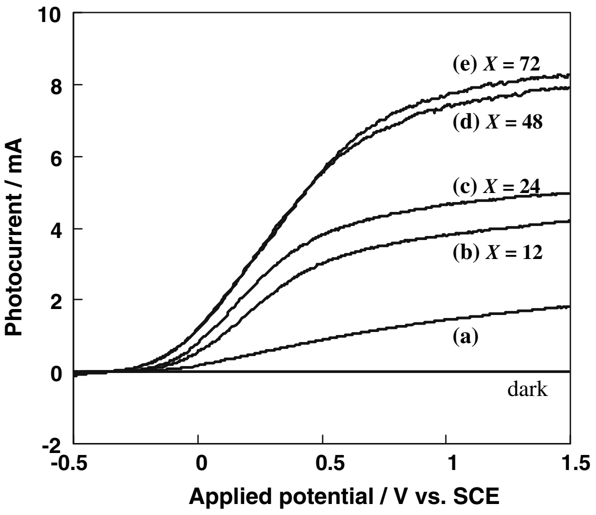

Fig. 3 Current–potential curves of (**a**) TiO_2/Ti and (**b**–**e**) nw-TiO_2(X)/Ti thin films. Light source: 500 W high pressure Hg lamp

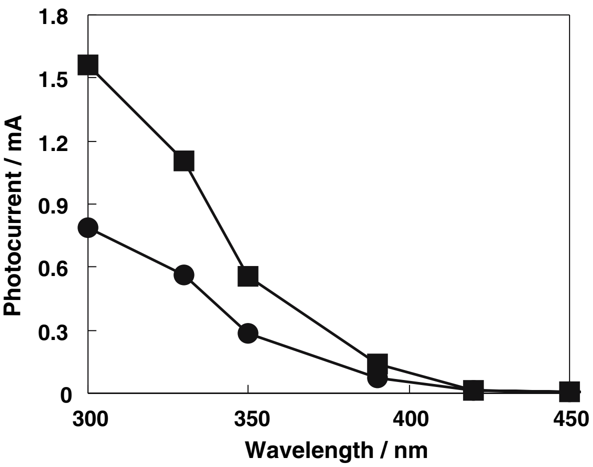

Fig. 4 The relative photocurrent as a function of the cut-off wavelength of incident light for (●) TiO_2/Ti and (■) nw-TiO_2(48)/Ti measured in 0.25 M K_2SO_4 aqueous solution at +1.0 V vs. SCE

The photocatalytic activity of TiO_2/Ti/Pt and nw-TiO_2(48)/Ti/Pt was investigated for the separate evolution of H_2 and O_2 from water under UV light irradiation. The TiO_2/Ti/Pt or nw-TiO_2(48)/Ti/Pt photocatalyst was mounted at the center of an H-type glass container, separating the two aqueous solutions, as shown in Fig. 5. A Nafion film was also mounted on the H-type glass container to provide the electrical connections which allowed the electron transfer between the two separated aqueous phases, playing the same role as a salt bridge between two aqueous phases. The TiO_2 side of the photocatalyst was immersed in 1.0 M NaOH and the Pt side was immersed in 0.5 M H_2SO_4 aqueous solution in order to add a small chemical bias to assist the electron transfer from the TiO_2 to Pt side through the metal substrate. Figure 6 shows the separate evolution reaction of H_2 and O_2 under irradiation with the full arc of a 500 W Xe lamp. Water was decomposed into H_2 and O_2 separately with a good linearity against the irradiation time and nw-TiO_2(48)/Ti/Pt exhibited much higher activity than TiO_2/Ti/Pt. It was, thus, clearly shown that the observed photocurrent is attributed not to the irreversible oxidation of nw-TiO_2(48)/Ti, but to the photoinduced oxidation of water to O_2. Previously, we showed that TiO_2 thin films which act as efficient photoanodes for the photoelectrochemical water splitting reaction also exhibit high photocatalytic activity for such significant reactions as the purification of toxic compounds in polluted water and air as well as the decomposition of water [24–26]. These results indicate that the nanowire TiO_2 thin film can act as an efficient photocatalyst for the decomposition of water for the separate evolution of H_2 and O_2 from H_2O under UV light irradiation. Highly active nanowire TiO_2 thin films could, thus, be easily prepared using low cost materials such as Ti foil.

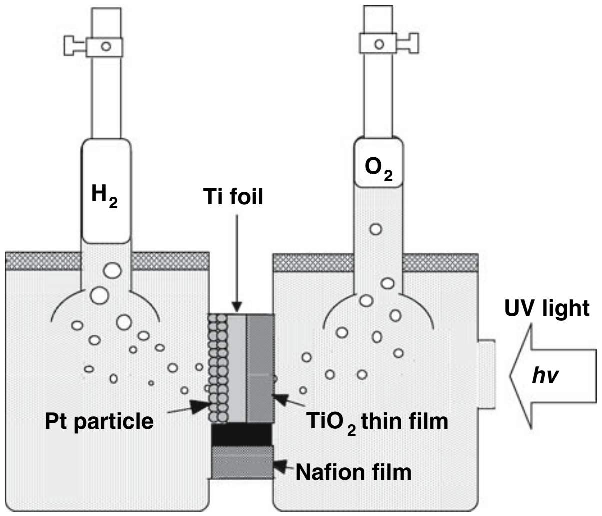

Fig. 5 H-type glass container for the separate evolution of H_2 and O_2 using a TiO_2/Ti/Pt thin film photocatalyst (TiO_2 side: 1.0 M NaOH aq; Pt side: 0.5 M H_2SO_4 aq)

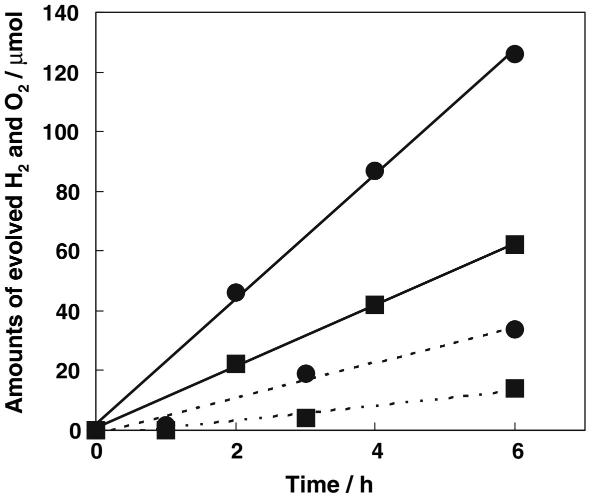

Fig. 6 Reaction time profiles of the separate evolution of (•) H_2 and (■) O_2 under irradiation with the full arc of a 500 W Xe lamp on nw-TiO_2(48)/Ti/Pt (solid line) and TiO_2/Ti/Pt (broken line) in an H-type glass container. Irradiation area: 10 × 20 mm^2

4 Conclusions

Nanowire TiO_2 thin films (nw-TiO_2/Ti) were synthesized by hydrothermal treatment of calcined Ti foil (TiO_2/Ti) in 10 M NaOH aqueous solution at 393 K. The surface area of nw-TiO_2/Ti was 15 times larger than that of TiO_2/Ti. The nw-TiO_2/Ti electrode was found to exhibit higher photocurrent than TiO_2/Ti due to the short diffusion length of the photoformed holes from the bulk to surface. Moreover, the nw-TiO_2/Ti photocatalyst exhibited higher photocatalytic reactivity for the separate evolution of H_2 and O_2 under UV light irradiation than TiO_2/Ti, thus, showing the potential for various applications as functional photocatalysts and photoelectrodes.

References

1. Hoffmann MR, Martin ST, Choi WY, Bahnemann DW (1995) Chem Rev 95:69
2. Anpo M (2004) Bull Chem Soc Jpn 77:1427
3. Anpo M, Dohshi S, Kitano M, Hu Y, Takeuchi M, Matsuoka M (2005) Annu Rev Mater Res 35:1
4. Anpo M, Shima T, Kodama S, Kubokawa Y (1987) J Phys Chem 91:4305
5. Sclafani A, Palmisano L, Schiavello M (1990) J Phys Chem 94:829
6. Zhang ZB, Wang CC, Zakaria R, Ying JY (1998) J Phys Chem B 102:10871
7. Kominami H, Murakami S, Kato J, Kera Y, Ohtani B (2002) J Phys Chem B 106:10501
8. Mills A, Porter G (1982) J Chem Soc Faraday trans 1 78:3659
9. Stone VF, Davis RJ (1998) Chem Mater 10:1468
10. Torimoto T, Nakamura N, Ikeda S, Ohtani B (2002) Phys Chem Chem Phys 4:5910
11. Kasuga T, Hiramatsu M, Hoson A, Sekino T, Niihara K (1998) Langmuir 14:3163
12. Kasuga T, Hiramatsu M, Hoson A, Sekino T, Niihara K (1999) Adv Mater 15:1307
13. Du GH, Chen Q, Che RC, Yuan ZY, Peng LM (2001) Appl Phys Lett 79:3702
14. Wang YQ, Hu GQ, Duan XF, Sun HL, Xue QK (2002) Chem Phys Lett 365:427
15. Tsai CC, Teng H (2004) Chem Mater 16:4352
16. Kavan L, Kalbac M, Zukalova M, Exnar I, Lorenzen V, Nesper R, Grätzel M (2004) Chem Mater 16:477
17. Yoshida R, Suzuki Y, Yoshikawa S (2005) J Solid State Chem 178:2179
18. Yuan ZY, Su BL (2004) Colloid Surf A-Physicochem Eng Asp 241:173
19. Adachi M, Murata Y, Yoshikawa S (2000) Chem Lett 8:942
20. Tian ZR, Voigt JA, Liu J, Mckenzie B, Xu H (2003) J Am Chem Soc 125:12384
21. Kitano M, Ueshima M, Matsuoka M, Anpo M (2006) In: Abstracts of spring meeting of Japan society of powder and powder metallurgy. The Japan Society of Powder and Powder Metallurgy, Tokyo, p 147
22. Yang SG, Quan X, Li XY, Sun C (2006) Photochem Photobiol Sci 5:808
23. Kikuchi H, Kitano M, Takeuchi M, Matsuoka M, Anpo M, Kamat PV (2006) J Phys Chem B 110:5537
24. Kitano M, Funatsu K, Matsuoka M, Ueshima M, Anpo M (2006) J Phys Chem B 110:25266
25. Kitano M, Tsujimaru K, Anpo M (2006) Appl Catal A Gen 314:179
26. Kitano M, Takeuchi M, Matsuoka M, Thomas JM, Anpo M (2007) Catal Today 120:133
27. Kavan L, Grätzel M, Gillbert SE, Klemenz C, Scheel HJ (1996) J Am Chem Soc 118:6716
28. Zhao JH, Wang AH, Green MA, Ferrazza F (1998) Appl Phys Lett 73:1991